J. Math. Computer Sci., 35 (2024), 411–430

Online: ISSN 2008-949X

Journal of Mathematics and Computer Science

Journal Homepage: www.isr-publications.com/jmcs

Optimizing $\mathcal{A}$-stable hyperbolic fitting for time efficiency: exploring constant and variable stepsize approaches

Dumitru Baleanu[a,*], Sania Qureshi[a,b], Amanullah Soomro[b], Mufutau Ajani Rufai[c]

[a]Department of Computer Science and Mathematics, Lebanese American University, P.O. Box 13-5053, Beirut, Lebanon.

[b]Department of Basic Sciences and Related Studies, Mehran University of Engineering & Technology, Jamshoro-76062, Pakistan.

[c]Dipartimento di Matematica, Università degli Studi di Bari Aldo Moro, 70125 Bari, Italy.

Abstract

This paper proposes an optimal time-efficient numerical method for solving the initial value problems (IVPs) of ordinary differential equations (ODEs) that is both $\mathcal{A}$-stable and hyperbolically fitted. The method is designed to handle both constant and variable step sizes, making it highly adaptable to different types of ODEs. The methodology proposed herein leverages the optimization of an off-grid point, derived from the predominant term of the local truncation error, to enhance both accuracy and stability in the solution of stiff ODEs. This approach incorporates a variable step size control, predicated upon the error estimation furnished by the embedded pair, and aims to minimize computational expenses while concurrently safeguarding both precision and stability. Furthermore, the stability domain of the proposed method is demonstrated to be optimal, signifying it encompasses the maximal conceivable set of step sizes wherein the method retains its stability. Other important measures including zero-stability, consistency, and convergence are also discussed theoretically and confirmed experimentally. Numerical experiments consisting of the Duffing system, sinusoidal stiff system, periodic orbit system, two-body system, Lorenz system, and the system for catenary equation demonstrate that the proposed method is highly competitive in terms of accuracy and efficiency, and outperforms several existing methods for solving stiff ODEs with both constant and variable step sizes.

Keywords: Stiff ODEs, stability, linear and non-linear IVPs, efficiency curves, optimized off-grid, local truncation error.

2020 MSC: 65L04, 65L05, 65L06, 65L20.

1. Introduction

The goal of this article is to provide an $\mathcal{A}$-stable optimal hyperbolically fitted approach for numerically solving the first-order IVPs of ODEs of the following form:

$$v'(x) = g(x, v(x)),\ v(x_0) = v_0,\ x \in [x_0, x_N], v, v_0 \in \mathbb{R}^m, g : \mathbb{R} \times \mathbb{R}^m \to \mathbb{R}^m, \tag{1.1}$$

where v_0 denotes the initial value of v at x_0, and g is considered to be sufficiently and adequately smooth that meets Lipchitz's condition, we can check that the existence and uniqueness theorem holds for the above IVP [20]. It may also be noted that the method we propose in this article is not limited to only

*Corresponding author
Email address: dumitru.baleanu@lau.edu.lb (Dumitru Baleanu)

doi: 10.22436/jmcs.035.04.03

Received: 2024-02-18 *Revised:* 2024-03-15 *Accepted:* 2024-03-30

first-order IVPs and can be used for finding approximate solutions to differential systems expressed in higher-order ODEs. It is also worth noting that the importance of differential equations cannot be denied as such equations appear almost in every field of science and engineering, for example see [3, 4, 14, 15, 21, 24, 25, 29, 32, 37, 44, 48, 52, 54] and many of the references cited therein.

According to Ramos and Rufai [39], IVPs of the kind in (1.1) have attracted the interest of many scholars in the field of numerical analysis since researchers commonly use them to model real-life application problems in biology, chemistry, engineering, physics and economics, among other social and natural sciences. For example, the world has recently witnessed the trauma brought by COVID-19 strains. More than a thousand models in the form of ODEs have been recently proposed by several researchers working in epidemiology to comprehend the transmission dynamics of the virus. A second-order differential equation explaining the behavior of a mass-spring-damper system with free and forced vibration is a fundamental model for engineers in mechanical and mechatronic engineering. Likewise, a second-order differential equation can be investigated numerically to understand the current flow in an RLC series circuit. Other models include logistic growth, kinetic reactions, fluid flow, weather prediction with Lorenz's system of three nonlinear ODEs, predator-prey models in ecology, and several others that require numerical treatment, thereby using solvers for the approximate solutions. Several PDEs arising in physical phenomena [2, 5, 6, 8–11, 19, 23, 31, 36, 50, 55] can also be dealt with the block methods.

Shortly after introducing calculus, it was realized that not all IVPs could be solved analytically as mentioned in [18]. As a result, numerical methods were developed to provide an approximate solution to the class of IVPs presented in (1.1). Some classical methods including Runge-Kutta methods, multi-step methods, and finite difference methods are discussed in [17]. Several scholars have developed various iterative techniques for numerically integrating different kinds of differential systems. For example, the authors in [43] have developed an efficient third-derivative hybrid block approach for integrating second-order two-point BVPs with Dirichlet, Neumann, or Robin boundary conditions. A method was developed using interpolation and collocation. The method considers two off-step optimal locations in a two-step block corresponding to a generic interval using a constructive approach. The approach gives an approximation for the whole integration interval. Numerical experiments showed the scheme's effectiveness. In [22], trigonometrically fitted two-step hybrid approaches for second-order initial value problems are considered. These approaches are ideal for the numerical integration of periodic or oscillatory problems with variable coefficients. Adding more parameters at each stage modifies two-step hybrid algorithms. In a recently published paper [41], the authors presented a two-step implicit hybrid block technique with fourth derivatives for linear and nonlinear third-order ODE boundary value problems. The developed method was derived using collocation and interpolation, and its convergence was seventh-order accurate. Solving an algebraic system of equations yielded discrete approximations at grid locations. Numerical studies showed that the proposed method gives accurate approximations that are better than some older methods and match well with analytical answers that are already known. Most recently, in [38], a consistent, accurate, stable, and time-efficient convergent approach has been described. The novel technique works for ODEs. Three intra-step grid points are optimized, including a detailed discussion of order stars. The new method outperforms the Lobatto III family of iterative methods. In the present article, we develop an optimized $\mathcal{A}$-stable hyperbolically fitted method (OAHFM) using both constant and variable stepsizes implementations to give a numerical solution to IVP systems of the type in (1.1).

The article is structured as follows. Section 2 provides step-by-step derivation for the suggested method while using interpolation and collocation techniques. Section 3 presents a theoretical analysis of the proposed method, including local truncation error, zero- and absolute stability, consistency, and convergence. The proposed method is also formulated using the variable stepsize approach that is described in Section 4. Some applied differential systems are simulated with the proposed and other competitive existing methods in Section 5. The concluding remarks, including some areas for future work, are reported in Section 6.

2. Mathematical formulation

Assuming we have a scalar equation of the type $v'(x) = g(x, v(x))$ and that a fitted function $\mathcal{I}(x, u)$, including an unknown parameter u that can approximate the true solution $v(x)$, we can proceed to solve the IVP in Eq.(1.1). In the forthcoming discussion, it will be demonstrated that the coefficients of the fitted function $\mathcal{I}(x, u)$ may be expressed in terms of v (the dependent variable), and g (the first-order derivative), computed at different mesh points. The proposed hyperbolically fitted method will be designed in such a way that its coefficients would be the terms that bring out the method capable enough to exactly integrate the given differential model when the required solutions belong to the linear space spanned by the basis function $P = \{1, x, \sinh(\omega x), \cosh(\omega x)\}$. Customarily, the symbols v_j , $g_j = g(x_j, v_j)$ are approximations of the true values $v(x_j)$ and $v'(x_j) = g(x_j, v(x_j))$, respectively, where $g(x, v(x)) = v'(x)$, $x_j = x_0 + jh$, $j = 1, 2 \ldots N$, with $x_0 = a, x_N = b$ and $h = \dfrac{x_N - x_0}{N}$, where h stands for the stepsize. We consider that the true solution $v(x)$ can be approximated by a fitted interpolating function $\mathcal{I}(x, u)$ defined by

$$v(x) \approx \mathcal{I}(x, u) = \alpha_0 + \alpha_1 x + \alpha_2 \sinh(\omega x) + \alpha_3 \cosh(\omega x),$$

where $\alpha_j, j = 0, 1, 2, 3$ are coefficients to be uniquely determined. When this approximation is taken into account, the following system of four equations is satisfied:

$$\mathcal{I}(x_n, u) = v_n, \quad \mathcal{I}'(x_{n+j}, u) = g_{n+j}, \quad j = 0, r, 1,$$

where the parameter u is given by $u = \omega h$ and r is an off-grid point to be optimized. We further consider the vector given as: $J = (v_n, g_n, g_{n+r}, g_{n+1})^T$, and the basis $P = \{1, x, \sinh(\omega x), \cosh(\omega x)\}$. As a result, we can now express the above system in the following matrix form:

$$W = \begin{pmatrix} 1 & x_n & \sinh(\omega x_n) & \cosh(\omega x_n) \\ 0 & 1 & \omega \cosh(\omega x_n) & \omega \sinh(\omega x_n) \\ 0 & 1 & \omega \cosh(\omega x_{n+r}) & \omega \sinh(\omega x_{n+r}) \\ 0 & 1 & \omega \cosh(\omega x_{n+1}) & \omega \sinh(\omega x_{n+1}) \end{pmatrix}.$$

It is then possible to explain the continuous approximation required for obtaining the proposed method in terms of the following equation:

$$\mathcal{I}(x, u) = \sum_{j=0}^{3} \frac{\det(W_j)}{\det(W)} P_j(x), \tag{2.1}$$

where W_j is the result of replacing the j^{th} column of W with J. The proof for the preceding discussion can be easily obtained by referring to the research work conducted by Abdulganiy et al. in [1]. Moreover, the Eq. (2.1) gives a continuous approximation to the true solution of the IVP (1.1) in the following form:

$$\mathcal{I}(x, u) = v_n + h\Big(\xi_{0,1}(x, u) g_n + \xi_{r,1}(x, u) g_{n+r} + \xi_{1,1}(x, u) g_{n+1}\Big). \tag{2.2}$$

The above continuous form (2.2) is evaluated at $x = x_{n+1}$ and the main method has the form

$$v_{n+1} = v_n + h\Big(\xi_{0,1}(u) g_n + \xi_{r,1}(u) g_{n+r} + \xi_{1,1}(u) g_{n+1}\Big), \tag{2.3}$$

while the additional method for (2.2) when evaluated at $x = x_{n+r}$ will be as follows:

$$v_{n+r} = v_n + h\Big(\xi_{0,r}(u) g_n + \xi_{r,r}(u) g_{n+r} + \xi_{1,r}(u) g_{n+1}\Big). \tag{2.4}$$

The coefficients in the main formula are found to be:

$$\begin{aligned}
\xi_{0,1} &= \frac{((-u\sinh(u)+\cosh(u)-1)\cosh(ur)+(u\cosh(u)-\sinh(u))\sinh(ur)+\cosh(u)-1)}{(-\sinh(u)\cosh(ur)+(\cosh(u)-1)\sinh(ur)+\sinh(u))u},\\
\xi_{r,1} &= \frac{(u\sinh(u)-2\cosh(u)+2)}{((\cosh(u)-1)\sinh(ur)-\sinh(u)(\cosh(ur)-1))u},\\
\xi_{1,1} &= -\frac{((u-\sinh(u))\sinh(ur)+(\cosh(ur)-1)(\cosh(u)-1))}{((\cosh(u)-1)\sinh(ur)-\sinh(u)(\cosh(ur)-1))u},
\end{aligned} \tag{2.5}$$

while the coefficients in the additional formula are found to be:

$$\begin{aligned}
\xi_{0,r} &= \frac{(-ru\sinh(u)-\cosh(u)-1)\cosh(ru)+(ru\cosh(u)+\sinh(u))\sinh(ru)+\cosh(u)+1}{u(-\cosh(ru)\sinh(u)+(\cosh(u)-1)\sinh(ru)+\sinh(u))},\\
\xi_{r,r} &= \frac{(\cosh(u)-1)\cosh(ru)+ru\sinh(u)-\sinh(u)\sinh(ru)-\cosh(u)+1}{u(-\cosh ru)\sinh(u)+(\cosh(u)-1)\sinh(ru)+\sinh(u))},\\
\xi_{1,r} &= \frac{-\sinh(ru)ru+2\cosh(ru)-2}{u((\cosh(u)-1)\sinh(ru)-(\cosh(ru)-1)\sinh(u))}.
\end{aligned} \tag{2.6}$$

Upon substitution of the coefficients determined above, the additional (2.4) and the main (2.3) formulae respectively get the following structure:

$$\begin{aligned}
v_{n+r} = v_n &+ \frac{g_n\,((-ru\sinh(u)-\cosh(u)-1)\cosh(ru)+(ru\cosh(u)+\sinh(u))\sinh(ru)+\cosh(u)+1)}{u(-\cosh(ru)\sinh(u)+(\cosh(u)-1)\sinh(ru)+\sinh(u))}\\
&+ \frac{g_{n+r}\,((\cosh(u)-1)\cosh(ur)+ur\sinh(u)-\sinh(ur)\sinh(u)-\cosh(u)+1)}{u(-\cosh(ur)\sinh(u)+(\cosh(u)-1)\sinh(ur)+\sinh(u))}\\
&+ \frac{g_{n+1}\,(-\sinh(ur)ru+2\cosh(ur)-2)}{u((\cosh(u)-1)\sinh(ur)-(\cosh(ur)-1)\sinh(u))}
\end{aligned} \tag{2.7}$$

and

$$\begin{aligned}
v_{n+1} = v_n &- \frac{g_n\,((-u\sinh(u)+\cosh(u)-1)\cosh(ur)+(u\cosh(u)-\sinh(u))\sinh(ur)+\cosh(u)-1)}{u(-\cosh(ur)\sinh(u)+(\cosh(u)-1)\sinh(ur)+\sinh(u))}\\
&+ \frac{g_{n+r}\,(u\sinh(u)-2\cosh(u)+2)}{u((\cosh(u)-1)\sinh(ur)-(\cosh(ur)-1)\sinh(u))}\\
&+ \frac{g_{n+1}\,((-u+\sinh(u))\sinh(ur)-(\cosh(u)-1)(\cosh(ur)-1))}{u((\cosh(u)-1)\sinh(ur)-(\cosh(ur)-1)\sinh(u))}.
\end{aligned} \tag{2.8}$$

The local truncation error (LTE) of the main formula (v_{n+1}) for the above-proposed method is as follows:

$$\begin{aligned}
\mathrm{LTE} = &\left(r\left(v^{(4)}(x_n)-\omega^2 v''(x_n)\right)+\frac{1}{2}\left(\omega^2 v''(x_n)-v^{(4)}(x_n)\right)\right)\frac{h^4}{36}\\
&+\left(\left(-\frac{\omega^2 v'''(x_n)}{12}+\frac{v^{(5)}(x_n)}{12}\right)r^2+\left(-\frac{\omega^2 v'''(x_n)}{12}+\frac{v^{(5)}(x_n)}{12}\right)r\right.\\
&\left.+\frac{\omega^2 v'''(x_n)}{15}-\frac{v^{(5)}(x_n)}{15}\right)\frac{h^5}{12}+\mathcal{O}(h^6).
\end{aligned} \tag{2.9}$$

After equating to zero the coefficients of h^4 in the above formula and solving the resulting equation, the following optimal value of the parameter r is found: $r=\frac{1}{2}$. Upon substitution of $r=1/2$ in Eq. (2.9), the main term of LTE has the following structure:

$$\mathrm{LTE}=\frac{1}{2880}\left(\omega^2 v'''(x_n)-v^{(5)}(x_n)\right)h^5+\mathcal{O}(h^6).$$

Finally, the obtained parameter r when substituted in Eqs. (2.7) and (2.8) yielded the following one-step optimized proposed hyperbolically fitted method with one intra-step point being optimal:

$$\begin{aligned} v_{n+r} &= v_n + \frac{h}{u(-2\sinh(\frac{u}{2})+\sinh(u))}\begin{pmatrix} \left(-\frac{u\sinh(\frac{u}{2})}{2}+\cosh(u)-2\cosh(\frac{u}{2})+1\right)g_n \\ +\left(1-\cosh(u)+\frac{u\sinh(u)}{2}\right)g_{n+r} \\ +\left(-\frac{u\sinh(\frac{u}{2})}{2}-2+2\cosh(\frac{u}{2})\right)g_{n+1} \end{pmatrix}, \\ v_{n+1} &= v_n + \frac{h}{u(-2\sinh(\frac{u}{2})+\sinh(u))}\begin{pmatrix} \left(-u\sinh(\frac{u}{2})+\cosh(u)-1\right)g_n \\ +\left(2-2\cosh(u)+u\sinh(u)\right)g_{n+r} \\ +\left(-u\sinh(\frac{u}{2})+\cosh(u)-1\right)g_{n+1} \end{pmatrix}. \end{aligned} \tag{2.10}$$

The pseudocode for the above-devised method (2.10) is explained in the Algorithm 1.

Algorithm 1: A pseudocode for the proposed optimized hyperbolically fitted method given in (2.10).

Data: x_0, x_N (integration interval), N (number of steps), $u = \omega h$, we choose parameter ω, v_0 (initial values), g.
Result: **sol** (discrete approximate solution of the IVP (1.1)).

Let $n = 0$, $h = \frac{x_N - x_0}{N}$.
Let $x_n = x_0, v_n = v_0$.
Let **sol** $= \{(x_n, v_n)\}$.
Solve (2.10) to obtain v_{n+k}, where $k = 0, r, 1$.
Let **sol** = **sol** $\cup\{(x_{n+k}, v_{n+k})\}_{k=0,r,1}$.
Let $x_n = x_n + h, v_n = v_{n+1}$.
Let $n = n + 1$,
if $n = N$ **then**
  go to 13
else
  go to 4;
end
End

3. Theoretical analysis

This section is devoted to the abstract analysis of the proposed optimized hyperbolically fitted method given in (2.10). The discussion consists of the derivation of the local truncation error of (2.10), consistency, order of convergence, and stability analysis, including both zero and absolute stability.

3.1. Local truncation error and consistency

The Taylor series is used for small values of u (see Lambert [28]). Thus the coefficients in (2.5) up to $O(u^{18})$ can be expressed as follows:

$$\begin{aligned} \xi_{0,1} &= \frac{h}{6} - \frac{hu^2}{720} + \frac{hu^4}{80640} - \frac{hu^6}{9676800} + \frac{hu^8}{1226244096} - \frac{691\,hu^{10}}{111588212736000} + \frac{hu^{12}}{21862180454400} \\ &\quad - \frac{3617\,hu^{14}}{10926717791109120000} + \frac{43867\,hu^{16}}{1860164436758416588800 0} - \frac{174611\,hu^{18}}{10523215956519042416640000}, \\ \xi_{r,1} &= \frac{2}{3}h + \frac{hu^2}{360} - \frac{hu^4}{40320} + \frac{hu^6}{4838400} - \frac{hu^8}{613122048} + \frac{691\,hu^{10}}{55794106368000} - \frac{hu^{12}}{10931090227200} \end{aligned}$$

$$+\frac{3617\,hu^{14}}{5463358895554560000}-\frac{43867\,hu^{16}}{9300822183792082944000}+\frac{174611\,hu^{18}}{526160797825952120832000},$$

$$\xi_{1,1}=\frac{h}{6}-\frac{hu^2}{720}+\frac{hu^4}{80640}-\frac{hu^6}{9676800}+\frac{hu^8}{1226244096}-\frac{691\,hu^{10}}{111588212736000}+\frac{hu^{12}}{21862180454400}$$
$$-\frac{3617\,hu^{14}}{10926717791109120000}+\frac{43867\,hu^{16}}{1860164436758416588800}-\frac{174611\,hu^{18}}{1052321595651904241664000}.$$

It is interesting to note that as $u\to 0$ in the power series expansion of the coefficients, methods based on the polynomial basis are recovered (Lambert [28]). As a result, we can write down the local truncation errors (LTEs) for the additional and main methods, respectively, as follows:

$$\mathrm{LTE}(v_{n+r},h)=-\frac{1}{384}\left(\omega^2v''(x_n)-v^{(4)}(x_n)\right)h^4,\quad \mathrm{LTE}(v_{n+1},h)=\frac{1}{2880}\left(\omega^2v'''(x_n)-v^{(5)}(x_n)\right)h^5.$$

The optimal proposed method is constructed by combining (2.3) and (2.4), where the coefficients of the method are explicitly given by (2.5) and (2.6). We describe the block-by-block procedure for calculating the series of vectors $V_0, V_1, \ldots$ in sequence (see [27]). Let the μ vector ($\mu=2$ is the number of points within the block) $V_\mu, V_{\mu-1}, G_\mu$, and $G_{\mu-1}$ be given as $V_\mu=(v_{n+r},v_{n+1})^T, V_{\mu-1}=(v_{n-1},v_n)^T, G_\mu=(g_{n+r},g_{n+1})^T$, and $G_{\mu-1}=(g_{n-1},g_n)^T$, then the 1-block 2-point method for (1.1) is given by

$$V_\mu=\sum_{i=1}^{1}\mathcal{A}^{(i)}V_{\mu-i}+\sum_{i=0}^{1}\mathcal{B}^{(i)}G_{\mu-i},$$

where $\mathcal{A}^{(i)}$ and $\mathcal{B}^{(i)}$ $(i=0,1)$ are 2×2 matrices whose entries are determined by the coefficients of (2.10).

3.2. Zero stability

Zero stability is a property of a numerical method for solving an IVP that determines how well the method approximates the solution as the time step size goes to zero. Specifically, a numerical method for solving an IVP is said to be zero-stable if the numerical solution approaches the exact solution as the time step size approaches zero for any initial condition. In other words, if the method is zero stable, then small errors in the initial conditions and in the numerical approximations at each time step do not accumulate and cause the numerical solution to diverge from the true solution over time. Zero stability is an important property for numerical methods for solving IVPs since it guarantees that the numerical solution will converge to the exact solution as the time step size becomes smaller. This property is typically analyzed using the concept of the stability region or stability function, which describes the region of the complex plane in which the numerical method remains bound for a given time step size. Mathematically, the following definition can be used:

Definition 3.1. The optimal hyperbolically fitted method (2.10) is zero stable provided the roots $\mathcal{R}_j, j=1,2$ of the first characteristic polynomial $\sigma(\mathcal{R})$ specified by

$$\sigma(\mathcal{R})=\det\left[\sum_{i=0}^{1}A^{(i)}\mathcal{R}^{1-i}\right]=0,\quad \mathcal{A}^{(0)}=-I, \tag{3.1}$$

satisfy $|\mathcal{R}_j|\leqslant 1, j=1,2$ and for those roots with $|\mathcal{R}_j|=1$, the multiplicity does not exceed 1 (see [34]). The optimal hyperbolically fitted method (2.10) is consistent as it has order $p>1$. We see from (3.1) and Definition 3.2 that optimal hyperbolically fitted method (2.10) is zero-stable since $\sigma(\mathcal{R})=\mathcal{R}(\mathcal{R}-1)=0$ satisfies $|\mathcal{R}_j|\leqslant 1, j=1,2$, and for those roots with $|\mathcal{R}_j|=1$, the multiplicity does not exceed 1. The optimal hyperbolically fitted method (2.10) is thus convergent, as zero-stability + consistency implies convergence.

3.3. Absolute stability analysis

It is preferable for numerical methods to be stable. Whether or not errors introduced at one step propagate to subsequent ones is a measure of a numerical method's stability. The error analysis of a

numerical method when applied to a simple initial-value problem of the type

$$v'(x) = \beta v(x),\ v(0) = v_0,\ \beta \in \mathbb{C} \quad \text{with} \quad \mathrm{Re}(\beta) < 0, \tag{3.2}$$

serves as a model for stability analysis. Since the exact answer $v(x) = v_0 \exp(\beta x)$ tends towards zero (since $\mathrm{Re}(\beta) < 0$) in an exponential way, the error should also tend towards zero as x (> 0) gets big enough. If a method does not work well with model (3.2), it probably won't work well with other initial-value problems either. To analyze the linear stability of the proposed optimal hyperbolically fitted method, we use the test equation (3.2) that results in

$$V_\mu = \mathcal{M}(z;u)V_{\mu-i},$$

where

$$\mathcal{M}(z;u) = \left(\mathcal{A}^{(0)} - z\mathcal{B}^{(0)}\right)^{-1}\left(\mathcal{A}^{(1)} + z\mathcal{B}^{(1)}\right),$$

where the matrix $\mathcal{M}(z;u)$ is the amplification matrix. The amplification matrix represents the linearized relationship between the approximation errors at two successive time steps. It measures the rate of increase or decrease in errors across successive iterations of a numerical algorithm. The stability of the approach can be checked by looking at the eigenvalues of the amplification matrix.

Definition 3.2 ([1])**.** In the $z-u$ plane, stability occurs when the spectral radius of $\mathcal{M}(z;u)$ is less than or equal to one, denoted by the inequality $|\rho[\mathcal{M}(z;u)]| \leqslant 1$. It is easily seen that the eigenvalues of $\mathcal{M}(z;u)$ are as follows:

$$\lambda_1 = 0, \quad \lambda_2 = \frac{\left((-z-2)u^2 + 2z^2\right)\sinh\left(\frac{u}{2}\right) - \cosh\left(\frac{u}{2}\right)uz^2}{\left((z-2)u^2 + 2z^2\right)\sinh\left(\frac{u}{2}\right) - \cosh\left(\frac{u}{2}\right)uz^2}.$$

Now, in order to study the stability characteristics of the method (2.10), we consider the spectral radius $\rho[\mathcal{M}(z;u)]$ of the amplification matrix given by

$$\rho[\mathcal{M}(z;u)] = \frac{\left((-z-2)u^2 + 2z^2\right)\sinh\left(\frac{u}{2}\right) - \cosh\left(\frac{u}{2}\right)uz^2}{\left((z-2)u^2 + 2z^2\right)\sinh\left(\frac{u}{2}\right) - \cosh\left(\frac{u}{2}\right)uz^2}. \tag{3.3}$$

The above rational function, when plotted, produced the Figure 1 wherein the left-half $z-u$ complex plane is covered for $z \in [-15, 15]$ and $u \in [-\pi, \pi]$. Indeed, the entire left half of the said plane will be covered by the rational function (3.3). This feature guarantees the absolute $\mathcal{A}$-stability [49] of the proposed optimal hyperbolically fitted method given in (2.10). Similar approaches to prove $\mathcal{A}$-stability of numerical methods have been adopted in several existing research works; for example, see [1, 7] and most of the references cited therein.

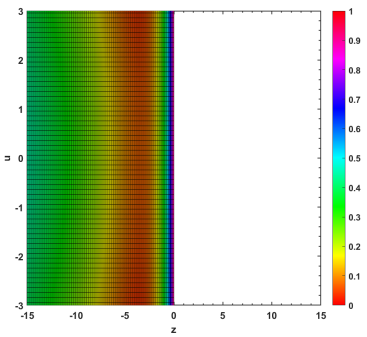

Figure 1: The plot of the absolute stability region ($\mathcal{A}$-stable) for the optimized hyperbolically fitted method given in (2.10).

4. Variable stepsize formulation

It is well known that the best performance of a numerical method occurs when a variable stepsize formulation is employed. Therefore, variable stepsize, which is based on a lower-order method for determining the local error at each block's endpoint $[x_n, x_{n+1}]$, must be considered. To formulate the adaptive stepsize, one has to consider a lower-order method for estimating the local error at the endpoint of each block. For the proposed implicit block method and the other methods taken for comparison, the second-order Runge-Kutta (RK) implicit method, called the Trapezoidal method, is used as an embedded method. This lower order method is considered keeping in mind the number of function evaluations in the simultaneous implementation of both methods. As a result, the computational cost of this embedding-like method will not increase in terms of the number of function evaluations. If a fitted method is chosen then it may bring additional function evaluations and does not serve the purpose of a variable stepsize approach. There are several existing block-type methods as well as trigonometrically fitted methods that use an adaptive stepsize approach and use a non-fitted method for the embedding purpose (see, for example, [40, 42]).

The difference between the approximate solutions obtained by the higher-order method and those found by the lower-order method will be employed as an error estimate (est) for the local error, which will then be used to determine the suitable stepsize of the new step. As a result, in order to measure the performance of the next step, we consider the following condition:

$$h_{new} = \Psi h_{old} \left(\frac{tol}{||est||} \right)^{\frac{1}{s+1}}, \tag{4.1}$$

where s is an order of the lower order method, and $0 < \Psi < 1$, is called the safety factor. The safety factor's main goal is to prevent excessive deviations in the new step. The safety factor chosen during the simulations in the present study is $\Psi = 0.95$. The abbreviation "tol" stands for "tolerance defined by the user." In the method's execution, we also impose the following conditional structure:

$$\textbf{If} \quad h_{min} \leqslant h_{new} \leqslant h_{max} \quad \textbf{then} \quad h_{old} = h_{new}.$$

The following simple steps can be used to express the above-stated criterion.

1. Take the first step-size and use the block approach to approximate the solution at grid points x_{n+r} and x_{n+1} using the information about the solution at x_n.
2. Use the known solution at grid point x_n to approximate the solution at grid point x_{n+1} using the trapezoidal method of the second order.
3. Estimate the local error by considering the difference $est = \|v_{n+1} - v^*_{n+1}\|$, where v_{n+1} and v^*_{n+1} denote the values obtained by the second order trapezoidal method and the block method (2.10) respectively at the grid point x_{n+1}.
4. If $est \leqslant tol$, where tol is the user's predefined tolerance, then we take $h_{new} = 2h_{old}$, that is, double the step-size to save the time and proceed the integration process with this h_{new} provided that $h_{min} \leqslant h_{new} \leqslant h_{max}$.
5. If $est > tol$, then revise the current step-size as given in the condition (4.1). In this case, return to the previous step and redo the computation with this new step-size h_{new} provided that $h_{min} \leqslant h_{new} \leqslant h_{max}$.

Different methods are employed in the scientific literature to choose the correct size of the initial step, which we refer to as "h_{ini}". For example, see [45, 46]. On the other hand, if a small h_{ini} is chosen (see [53]), the algorithm will automatically redefine it if it is needed.

5. Numerical simulations

In this segment of the scholarly investigation, numerical simulations were executed for various IVP models that emerge in the disciplines of science and engineering. These models were solved employing the devised $\mathcal{A}$-stable hyperbolically fitted methodology, as specified in equation (2.10), achieving a minimum third-order convergence. This was accomplished through the utilization of both constant and adaptive stepsize strategies. For the purpose of comparative analysis, the classical implicit Rad-II method [12] from the Radau family, recognized for its third-order convergence, was selected. Additionally, two other numerical methods, namely the Jator and FESDIRK methods which are characterized by their trigonometrically fitted approach and fourth-order convergence, were selected for comparison from [33] and [35], respectively. The comparative evaluation was based on various metrics of absolute errors, including the normed error ($||NE||_\infty$), the root mean square error (RMSE), the number of function evaluations (FEE), the absolute average error (Mean), the number of steps (N), and the precision factor (scd). In the scenario involving variable stepsize simulations, differing tolerance values (ϵ) were taken into account. Moreover, efficiency curves for each method were delineated utilizing a variable stepsize approach. The computational formulae pertinent to the aforementioned metrics are outlined as follows:

$$||NE||_\infty = \max_{1\leqslant i\leqslant n}\left(\sum_{j=1}^{n}||v(x_{ij})-v_{ij}||\right), \qquad RMSE = \sqrt{\frac{\sum_{i=1}^{n}(v(x_i)-v_i)^2}{n}},$$

$$Mean = \frac{\sum_{i=1}^{n}|v(x_i)-v_i|}{n}, \qquad scd = -\log_{10}\left[\max_{1\leqslant i\leqslant n}||v(x_i)-v_i||\right].$$

For numerical computations, the software Mathematica 12.1 running on Windows OS having processor Intel(R) Core(TM) i7-1065G7 CPU @ 1.30GHz 1.50 GHz working with installed RAM of 24.0GB is used. Moreover, it may be noted that there are a number of trigonometrically-fitted approaches mentioned in the literature, but none of them provides a conclusive means of determining the optimum frequency ω [51]. Therefore, we have arbitrarily chosen the ω value while simulating the differential systems.

Problem 5.1. Consider the following scalar type first-order equation [18]

$$v_1'(x) = v_1(x)\cos(x), \qquad x \in [0\ 100], \quad \omega = 10. \tag{5.1}$$

The exact solution for the equation (5.1) is $v_1(x) = \exp(\sin x)$. The maximum absolute errors (MaxErr) are computed as shown in Table 1. It is observed that the errors decrease by four orders of magnitude as we increase the steps by one order of magnitude. This behavior of the errors shows that the effective order of accuracy of the proposed optimal method is four.

Table 1: The maximum absolute error for the Problem 5.1 with different number of steps N.

N	10^2	10^3	10^4
MaxErr	1.6083×10^{-2}	1.5294×10^{-6}	7.7427×10^{-10}

Problem 5.2. Consider the following two-dimensional non-homogeneous system given in [12]:

$$v_1'(x) = v_2(x), \quad v_2'(x) = -v_1(x) + x, \quad v_1(0) = 1, \quad v_2(0) = 2, \quad x \in [0\,1], \quad \omega = 2\pi.$$

The exact solution is $v_1(x) = \sin(x) + \cos(x) + x$, $v_2(x) = \cos(x) - \sin(x) + 1$. The above system is simulated with the optimized $\mathcal{A}$-stable hyperbolically fitted method given in (2.10) and other existing methods while taking different values for the number of steps N using both constant and adaptive stepsize strategies. As observed in Tables 2-4, the proposed approach (OAHFM) returned the smallest values of the absolute errors and highest values for the precision factors, leading to prove its better performance

in comparison to other methods. When the adaptive stepsize approach is used in Table 5 with different tolerances, the better performance of the proposed approach is confirmed not only in terms of the absolute errors but also for the factors like the number of steps, function evaluations, and precision factors. To check the time-efficiency of the proposed method, a plot of the efficiency curves is given in Figure 2 wherein the method in (2.10) takes the minimum amount of CPU time to yield the minor maximum global error in comparison to other methods.

Table 2: The error distributions and the precision factor (scd) for the Problem 5.2 with number of steps $N = 2^5$ using constant stepsize h.

Method	$\|\|NE\|\|_\infty$	RMSE	Mean	scd
OAHFM	6.5162×10^{-9}	4.7172×10^{-9}	3.9726×10^{-9}	8.186
Jator	7.0485×10^{-8}	5.1010×10^{-8}	4.2924×10^{-8}	7.152
FESDIRK	7.3812×10^{-8}	5.3435×10^{-8}	4.5004×10^{-8}	7.132
Rad-II	5.8667×10^{-7}	4.2382×10^{-7}	3.5471×10^{-7}	6.231

Table 3: The error distributions and the precision factor (scd) for the Problem 5.2 with number of steps $N = 2^6$ using constant stepsize h.

Method	$\|\|NE\|\|_\infty$	RMSE	Mean	scd
OAHFM	1.2860×10^{-9}	9.3140×10^{-10}	7.8542×10^{-10}	8.891
Jator	4.4024×10^{-9}	3.1860×10^{-9}	2.6807×10^{-9}	8.356
FESDIRK	9.2275×10^{-9}	6.6791×10^{-9}	5.6228×10^{-9}	8.035
Rad-II	7.3273×10^{-8}	5.2981×10^{-8}	4.4462×10^{-8}	7.135

Table 4: The error distributions and the precision factor (scd) for the Problem 5.2 with number of steps $N = 2^7$ using constant stepsize h.

Method	$\|\|NE\|\|_\infty$	RMSE	Mean	scd
OAHFM	2.9995×10^{-10}	2.1744×10^{-10}	1.8384×10^{-10}	9.523
Jator	2.7605×10^{-10}	2.0065×10^{-10}	1.7087×10^{-10}	9.559
FESDIRK	1.1535×10^{-9}	8.3487×10^{-10}	7.0268×10^{-10}	8.938
Rad-II	9.1552×10^{-9}	6.6227×10^{-9}	5.5653×10^{-9}	8.038

Table 5: The error distributions and the precision factor (scd) for the Problem 5.2 with initial stepsize $h_{ini} = 10^{-4}$ using variable stepsize approach.

ϵ	Method	$\|\|NE\|\|_\infty$	RMSE	Mean	N	FEE	scd
10^{-4}	OAHFM	1.8404×10^{-7}	1.3320×10^{-7}	1.1209×10^{-7}	12	36	6.735
	Jator	5.4910×10^{-6}	3.9735×10^{-6}	3.3427×10^{-6}	13	39	5.260
	FESDIRK	9.757×10^{-7}	7.0652×10^{-7}	5.9550×10^{-7}	15	60	6.011
	Rad-II	7.7460×10^{-6}	5.5822×10^{-6}	4.6347×10^{-6}	15	60	5.111
10^{-6}	OAHFM	2.2332×10^{-9}	1.6170×10^{-9}	1.3628×10^{-9}	52	156	8.651
	Jator	1.1435×10^{-8}	8.5089×10^{-9}	7.5911×10^{-9}	53	159	7.942
	FESDIRK	9.7235×10^{-9}	7.038×10^{-9}	5.9249×10^{-9}	65	260	8.012
	Rad-II	7.7173×10^{-8}	5.5799×10^{-8}	4.6824×10^{-8}	65	260	7.113
10^{-8}	OAHFM	8.9271×10^{-11}	6.4823×10^{-11}	5.5060×10^{-11}	234	702	10.049
	Jator2013	2.1945×10^{-9}	2.1233×10^{-9}	2.1220×10^{-9}	237	711	8.659
	FESDIRK	9.6714×10^{-11}	6.9995×10^{-11}	5.8904×10^{-11}	295	1180	10.015
	Rad-II	7.6728×10^{-10}	5.5517×10^{-10}	4.6688×10^{-10}	295	1180	9.115

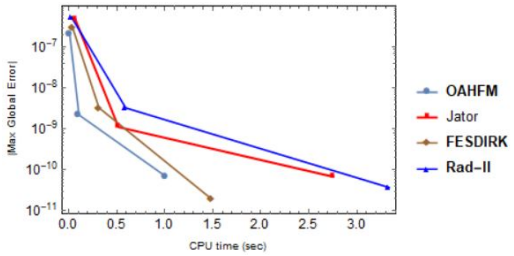

Figure 2: Comparison of the optimized $\mathcal{A}$-stable hyperbolically fitted method given in (2.10) with several other methods via efficiency curves of the absolute maximum global error versus CPU time (sec) on the logarithmic scale for the Problem 5.2 while matching the error to the tolerance 10^{-i}, where $i = 7, 9, 11$.

Problem 5.3. Consider the following nonlinear Duffing system as given in [26]:

$$v_1'(x) = v_2(x), \quad v_1(0) = 0.200426728067, \quad v_2'(x) = -v_1(x) - v_1(x)^3 - 0.002\cos(1.01x), \quad v_2(0) = 0,$$

where $x \in [0, 10]$, $\omega = 2\pi$ and the exact solution for the above Duffing system is given as follows:

$$\begin{aligned} v_1(x) &= 0.200179477536\cos(0.101x) + 0.246946143 \times 10^{-4}\cos(0.303x) + 0.304014 \times 10^{-7}\cos(0.505x) \\ &\quad + 0.374 \times 10^{-10}\cos(0.707x), \\ v_2(x) &= -0.2021812723\sin(0.101x) - 0.7482468133 \times 10^{-4}\sin(0.303x) - 0.153527070 \times 10^{-6}\sin(0.505x) \\ &\quad - 0.264418 \times 10^{-9}\sin(0.707x). \end{aligned}$$

The above highly stiff Duffing system is simulated with the optimized $\mathcal{A}$-stable hyperbolically fitted method given in (2.10) and other existing methods while taking different values for the number of steps N using both constant and variable stepsize strategies. As observed in Tables 6-8, the proposed approach (OAHFM) returned the smallest values of the absolute errors and highest values for the precision factors in each case, leading to prove its better performance in comparison to other methods. Furthermore, when the variable stepsize approach is used in Table 9 while taking different initial stepsize values h_{ini} and tolerances, the better performance of the proposed approach is further confirmed in terms of the absolute errors and the precision factors. The frequency factor for the present problem is set to $\omega = 2\pi$ during the simulations over the integration interval of length 10. To check the time-efficiency of the proposed method, a plot of the efficiency curves is given in Figure 3 wherein the method in (2.10) takes the minimum amount of CPU time to yield the minor maximum global error in comparison to other methods.

Table 6: The error distributions and the precision factor (scd) for the Problem 5.3 with number of steps $N = 2^5$ using constant stepsize h.

Method	$\|\|NE\|\|_\infty$	RMSE	Mean	scd
OAHFM	2.8269×10^{-5}	2.569×10^{-5}	2.5545×10^{-5}	4.549
Jator	1.1461×10^{-3}	1.043×10^{-3}	1.0373×10^{-3}	2.941
FESDIRK	1.0329×10^{-4}	9.6949×10^{-5}	9.6726×10^{-5}	3.986
Rad-II	8.1851×10^{-4}	7.6263×10^{-4}	7.6041×10^{-4}	3.087

Table 7: The error distributions and the precision factor (scd) for the Problem 5.3 with number of steps $N = 2^6$ using constant stepsize h.

Method	$\|\|NE\|\|_\infty$	RMSE	Mean	scd
OAHFM	1.9058×10^{-6}	1.817×10^{-6}	1.815×10^{-6}	5.711
Jator	6.6864×10^{-5}	6.0897×10^{-5}	6.0571×10^{-5}	4.175
FESDIRK	1.3093×10^{-5}	1.2153×10^{-5}	1.2114×10^{-5}	4.883
Rad-II	1.0287×10^{-4}	9.582×10^{-5}	9.5539×10^{-5}	3.988

Table 8: The error distributions and the precision factor (scd) for the Problem 5.3 with number of steps $N = 2^7$ using constant stepsize h.

Method	$\|\|NE\|\|_\infty$	RMSE	Mean	scd
OAHFM	3.8507×10^{-7}	2.9271×10^{-7}	2.6849×10^{-7}	6.415
Jator	4.1116×10^{-6}	3.8442×10^{-6}	3.8342×10^{-6}	5.386
FESDIRK	1.8783×10^{-6}	1.6501×10^{-6}	1.6315×10^{-6}	5.726
Rad-II	1.3128×10^{-5}	1.2128×10^{-5}	1.2082×10^{-5}	4.882

Table 9: The error distributions and the precision factor (scd) for the Problem 5.3 with different values of h_{ini} and tolerance ϵ using variable stepsize approach.

h_{ini}	ϵ	Method	$\|\|NE\|\|_\infty$	RMSE	Mean	scd
10^{-1}	10^{-2}	OAHFM	1.0775×10^{-3}	9.8501×10^{-4}	9.802×10^{-4}	2.968
		Jator	3.9218×10^{-2}	3.5961×10^{-2}	3.5798×10^{-2}	1.407
		FESDIRK	8.1236×10^{-4}	7.6457×10^{-4}	7.6297×10^{-4}	3.090
		Rad-II	6.3161×10^{-3}	5.8047×10^{-3}	5.7799×10^{-3}	2.191
10^{-2}	10^{-3}	OAHFM	5.7996×10^{-5}	5.254×10^{-5}	5.2225×10^{-5}	4.237
		Jator	2.1246×10^{-3}	1.9349×10^{-3}	1.9245×10^{-3}	2.673
		FESDIRK	8.7428×10^{-5}	8.1515×10^{-5}	8.1283×10^{-5}	4.058
		Rad-II	6.8792×10^{-4}	6.3984×10^{-4}	6.3788×10^{-4}	3.163
10^{-3}	10^{-4}	OAHFM	3.0465×10^{-6}	2.8394×10^{-6}	2.8312×10^{-6}	5.516
		Jator	1.0589×10^{-4}	9.6526×10^{-5}	9.6021×10^{-5}	3.975
		FESDIRK	9.2195×10^{-6}	8.4777×10^{-6}	8.442×10^{-6}	5.035
		Rad-II	7.1646×10^{-5}	6.6545×10^{-5}	6.6332×10^{-5}	4.145

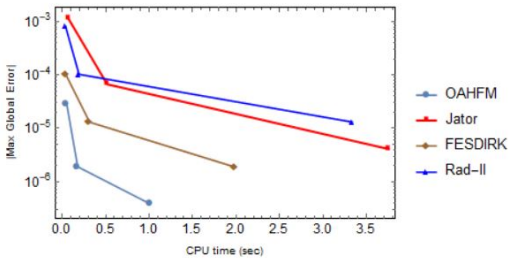

Figure 3: Comparison of the optimized $\mathcal{A}$-stable hyperbolically fitted method given in (2.10) with several other methods via efficiency curves of the absolute maximum global error versus CPU time (sec) on the logarithmic scale for the Problem 5.3.

Problem 5.4. The sinusoidal stiff system taken from [1] is given below:

$$\begin{aligned} v_1'(x) &= -2v_1(x) + v_2(x) + 2\sin(x), \\ v_2'(x) &= 998v_1(x) - 999v_2(x) + 999\cos(x) - 999\sin(x), \\ v_1(0) &= 2, \quad v_2(0) = 3, \quad x \in [0,5]. \end{aligned} \tag{5.2}$$

Exact solution is $v_1(x) = 2\exp(-x) + \sin(x)$, $v_2(x) = 2\exp(-x) + \cos(x)$, where $\omega = 4\pi$.

The above stiff sinusoidal system is simulated with the optimized $\mathcal{A}$-stable hyperbolically fitted method given in (2.10) and other existing methods while taking different values for the number of steps N using both constant and variable stepsize strategies. As observed in Tables 10-12, the proposed approach (OAHFM) returned the smallest values of the absolute errors and highest values for the precision factors in each case, leading to prove its better performance in comparison to other methods. Furthermore, when the variable stepsize approach is used in Table 13 while taking different initial stepsize values h_{ini} and

tolerances, the better performance of the proposed approach is further confirmed in terms of the absolute errors and the precision factors. It is worthy to be noted that the methods FESDIRK and standard Radau-II could not perform well enough using the constant stepsize strategy whereas both methods started to obtain reasonably small errors with their variable stepsize version. The frequency factor for this sinusoidal problem given in (5.2) is set to $\omega = 4\pi$ during the simulations over the integration interval of length 5. To check the time-efficiency of the proposed method, a plot of the efficiency curves is given in Figure 4 wherein the method in (2.10) takes the minimum amount of CPU time to yield the minor maximum global error in comparison to other methods.

Table 10: The error distributions and the precision factor (scd) for the Problem 5.4 with number of steps $N = 2^5$ using constant stepsize h.

Method	$\|NE\|_\infty$	RMSE	Mean	scd
OAHFM	1.2874×10^{-6}	1.2615×10^{-6}	1.2612×10^{-6}	5.890
Jator	1.7022×10^{-4}	1.5159×10^{-4}	1.5028×10^{-4}	3.769
FESDIRK	2.3627×10^{56}	1.6707×10^{56}	1.1825×10^{56}	-56.373
Rad-II	3.468×10^{57}	2.4523×10^{57}	1.7358×10^{57}	-57.540

Table 11: The error distributions and the precision factor (scd) for the Problem 5.4 with number of steps $N = 2^6$ using constant stepsize h.

Method	$\|NE\|_\infty$	RMSE	Mean	scd
OAHFM	8.6471×10^{-8}	8.3401×10^{-8}	8.3342×10^{-8}	7.063
Jator	1.0419×10^{-5}	9.1474×10^{-6}	9.0434×10^{-6}	4.982
FESDIRK	4.5412×10^{95}	3.2111×10^{95}	2.2729×10^{95}	-95.657
Rad-II	2.6175×10^{96}	1.8509×10^{96}	1.3101×10^{96}	-96.418

Table 12: The error distributions and the precision factor (scd) for the Problem 5.4 with number of steps $N = 2^7$ using constant stepsize h.

Method	$\|NE\|_\infty$	RMSE	Mean	scd
OAHFM	8.5004×10^{-9}	8.0004×10^{-9}	7.9837×10^{-9}	8.071
Jator	6.5311×10^{-7}	5.7001×10^{-7}	5.6281×10^{-7}	6.185
FESDIRK	3.5363×10^{145}	2.5005×10^{145}	1.7699×10^{145}	-145.550
Rad-II	6.3967×10^{151}	4.5231×10^{151}	3.2016×10^{151}	-151.810

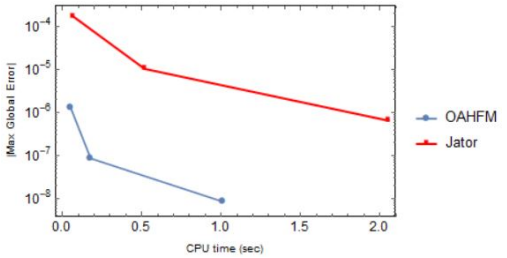

Figure 4: Comparison of the optimized $\mathcal{A}$-stable hyperbolically fitted method given in (2.10) with several other methods via efficiency curves of the absolute maximum global error versus CPU time (sec) on the logarithmic scale for the Problem 5.4.

Table 13: The error distributions and the precision factor (scd) for the Problem 5.4 with different values of h_{ini} and tolerance ϵ using variable stepsize approach.

h_{ini}	ϵ	Method	$\|NE\|_\infty$	RMSE	Mean	scd
10^{-1}	10^{-2}	OAHFM	8.9142×10^{-5}	8.6981×10^{-5}	8.6953×10^{-5}	4.041
		Jator	1.2764×10^{-3}	1.233×10^{-3}	1.2322×10^{-3}	2.894
		FESDIRK	3.2984×10^{-4}	2.3323×10^{-4}	1.6509×10^{-4}	3.482
		Rad-II	1.7832×10^{-4}	1.2617×10^{-4}	9.2307×10^{-5}	3.749
10^{-2}	10^{-3}	OAHFM	5.5058×10^{-6}	5.1088×10^{-6}	5.092×10^{-6}	5.259
		Jator	6.9961×10^{-5}	6.355×10^{-5}	6.3188×10^{-5}	4.155
		FESDIRK	2.5824×10^{-5}	1.8261×10^{-5}	1.2926×10^{-5}	4.588
		Rad-II	2.4837×10^{-4}	1.7583×10^{-4}	1.3017×10^{-4}	3.605
10^{-3}	10^{-4}	OAHFM	2.5488×10^{-7}	2.4599×10^{-7}	2.4582×10^{-7}	6.594
		Jator	7.0101×10^{-6}	6.0068×10^{-6}	5.9041×10^{-6}	5.154
		FESDIRK	2.7399×10^{-6}	1.9374×10^{-6}	1.3728×10^{-6}	5.562
		Rad-II	3.4986×10^{-5}	2.4878×10^{-5}	1.9346×10^{-5}	4.456

Problem 5.5 ([13]). The Lorenz system that describe a simplified model of atmospheric convection. Lorenz system includes three ordinary differential equations given below:

$$\begin{aligned} v_1'(x) &= \rho(v_1(x) - v_2(x)), & v_1(0) &= 1, \\ v_2'(x) &= v_1(x)(\sigma - v_3(x)) - v_2(x), & v_2(0) &= 1, \\ v_3'(x) &= v_1(x)v_2(x) - \beta v_3(x), & v_3(0) &= 1, \quad x \in [0, 0.5]. \end{aligned} \tag{5.3}$$

In these equations, v_1, v_2, and v_3 represent the state variables that describe the system's behavior over time. They correspond to the temperature difference, horizontal temperature variation, and vertical temperature variation, respectively. The parameters σ, ρ, and β are constants that control the system's dynamics. Typically, their values are set to $\rho = 10$, $\sigma = 28$, and $\beta = 83$. The system in (5.3) does not have a closed-form solution, so its reference solution $v_1 = -1.78252387338970$ $v_2 = 13.4806047749901$, and $v_3 = 3.60221303181254$ is used. The frequency factor for this Lorenz system problem 5.3 is set to $\omega = 20\pi$ during the simulations. It is clear from Tables 14 and 16 that the proposed (OAHFM) method outperforms the rest of the chosen methods at the final mesh point.

Table 14: The error distributions and the precision factor (scd) for the Problem 5.5 with number of steps $N = 2^5$ using constant stepsize h.

Method	Last Err $v_1(x)$	Last Err $v_2(x)$	Last Err $v_3(x)$
OAHFM	1.5989×10^{-4}	5.1196×10^{-4}	2.0892×10^{-4}
Jator	4.8637×10^{-3}	2.5773×10^{-3}	1.4885×10^{-3}
FESDIRK	1.7436×10^{-3}	2.8923×10^{-3}	1.412×10^{-3}
Rad-II	1.4159×10^{-2}	2.1237×10^{-2}	9.8373×10^{-3}

Table 15: The error distributions and the precision factor (scd) for the Problem 5.4 with number of steps $N = 2^6$ using constant stepsize h.

Method	Last Err $v_1(x)$	Last Err $v_2(x)$	Last Err $v_3(x)$
OAHFM	1.2557×10^{-5}	3.3562×10^{-5}	1.3722×10^{-5}
Jator	2.9881×10^{-4}	1.5962×10^{-4}	9.2228×10^{-5}
FESDIRK	2.1796×10^{-4}	3.5926×10^{-4}	1.7566×10^{-4}
Rad-II	1.7571×10^{-3}	2.748×10^{-3}	1.2746×10^{-3}

Table 16: The error distributions and the precision factor (scd) for the Problem 5.4 with number of steps $N = 2^7$ using constant stepsize h.

Method	Last Err $v_1(x)$	Last Err $v_2(x)$	Last Err $v_3(x)$
OAHFM	1.5667×10^{-6}	2.4403×10^{-6}	8.5735×10^{-7}
Jator	1.8416×10^{-5}	9.982×10^{-6}	5.9528×10^{-6}
FESDIRK	2.743×10^{-5}	4.4803×10^{-5}	2.2087×10^{-5}
Rad-II	2.1871×10^{-4}	3.4911×10^{-4}	1.6227×10^{-4}

Problem 5.6. Finally, consider the periodic orbit system taken from [47]:

$$v_1''(x) = -s_1(x) + \frac{\cos(x)}{1000}, \quad v_1(0) = 1, \quad v_1'(0) = 0,$$
$$v_2''(x) = -v_2(x) + \frac{\sin(x)}{1000}, \quad v_2(0) = 1, \quad v_2'(0) = \frac{9995}{10000}.$$

The exact solution for the periodic orbit system over the interval $[0, 1]$ is given as follows:

$$v_1(x) = \cos(x) + \frac{x\sin(x)}{2000}, \quad v_2(x) = \sin(x) - \frac{x\cos(x)}{2000}.$$

The above periodic orbit system is simulated with the optimized $\mathcal{A}$-stable hyperbolically fitted method given in (2.10) and other existing methods while taking different values for the number of steps N using both constant and variable stepsize strategies. As observed in Tables 17-19, the proposed approach (OAHFM) returned the smallest values of the absolute errors and highest values for the precision factors, leading to prove its better performance in comparison to other methods. These Tables further noted that third-order method (Rad-II) did not return acceptable values of the precision factor due to having a comparatively most significant normed error. Furthermore, when the variable stepsize approach is used in Table 20 while taking different initial stepsize values h_{ini} and tolerances, the better performance of the proposed approach is further confirmed in terms of the absolute errors and the precision factors. The frequency factor for the present problem is set to $\omega = 6\pi$. To check the time-efficiency of the proposed method, a plot of the efficiency curves is given in Figure 5 wherein the method in (2.10) takes the minimum amount of CPU time to yield the minor maximum global error in comparison to other methods.

Table 17: The error distributions and the precision factor (scd) for the Problem 5.6 with number of steps $N = 2^5$ using constant stepsize h.

Method	$\|NE\|_\infty$	RMSE	Mean	scd
OAHFM	3.9641×10^{-9}	3.3669×10^{-9}	3.301×10^{-9}	8.402
Jator	3.9766×10^{-7}	3.3797×10^{-7}	3.3141×10^{-7}	6.401
FESDIRK	4.4919×10^{-8}	3.8146×10^{-8}	3.7397×10^{-8}	7.348
Rad-II	1.2892	9.4742×10^{-1}	8.9056×10^{-1}	-0.110

Table 18: The error distributions and the precision factor (scd) for the Problem 5.6 with number of steps $N = 2^6$ using constant stepsize h.

Method	$\|NE\|_\infty$	RMSE	Mean	scd
OAHFM	7.8314×10^{-10}	6.6463×10^{-10}	6.5145×10^{-10}	9.106
Jator	2.4700×10^{-8}	2.0995×10^{-8}	2.0588×10^{-8}	7.607
FESDIRK	5.6120×10^{-9}	4.7684×10^{-9}	4.6755×10^{-9}	8.251
Rad-II	1.3149	9.6091×10^{-1}	9.0270×10^{-1}	-0.119

Table 19: The error distributions and the precision factor (scd) for the Problem 5.6 with number of steps $N = 2^7$ using constant stepsize h.

Method	$\|NE\|_\infty$	RMSE	Mean	scd
OAHFM	1.8298×10^{-10}	1.5501×10^{-10}	1.5185×10^{-10}	9.738
Jator	1.5399×10^{-9}	1.31×10^{-9}	1.2850×10^{-9}	8.813
FESDIRK	7.0134×10^{-10}	5.9602×10^{-10}	5.8444×10^{-10}	9.154
Rad-II	1.3278	9.6766×10^{-1}	9.0877×10^{-1}	-0.123

Table 20: The error distributions and the precision factor (scd) for the Problem 5.6 with different values of h_{ini} and tolerance ϵ using variable stepsize approach.

h_{ini}	ϵ	Method	$\|NE\|_\infty$	RMSE	Mean	scd
10^{-1}	10^{-2}	OAHFM	3.2940×10^{-10}	2.7667×10^{-10}	2.7028×10^{-10}	9.482
		Jator	5.3371×10^{-9}	4.4981×10^{-9}	4.3994×10^{-9}	8.273
		FESDIRK	5.9203×10^{-5}	5.2474×10^{-5}	5.1974×10^{-5}	4.228
		Rad-II	4.2836×10^{-4}	4.1224×10^{-4}	4.1192×10^{-4}	3.368
10^{-2}	10^{-3}	OAHFM	3.2349×10^{-12}	2.6416×10^{-12}	2.5520×10^{-12}	11.490
		Jator	4.1565×10^{-11}	3.6954×10^{-11}	3.6624×10^{-11}	10.381
		FESDIRK	7.3481×10^{-6}	6.3895×10^{-6}	6.3036×10^{-6}	5.134
		Rad-II	5.6278×10^{-5}	5.0772×10^{-5}	5.0434×10^{-5}	4.241
10^{-3}	10^{-4}	OAHFM	1.3756×10^{-13}	1.2419×10^{-13}	12.862×10^{-13}	12.875
		Jator	1.2956×10^{-8}	1.2001×10^{-8}	1.1960×10^{-8}	7.888
		FESDIRK	8.5686×10^{-7}	7.2272×10^{-7}	7.0702×10^{-7}	6.067
		Rad-II	6.6805×10^{-6}	5.7277×10^{-6}	5.6307×10^{-6}	5.175

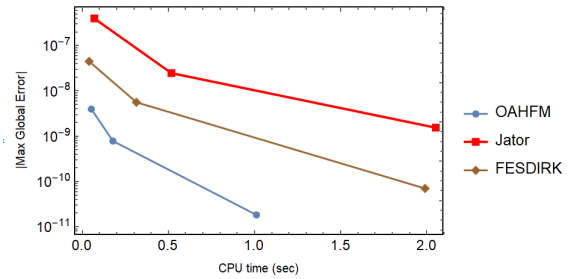

Figure 5: Comparison of the optimized $\mathcal{A}$-stable hyperbolically fitted method given in (2.10) with several other methods via efficiency curves of the absolute maximum global error versus CPU time (sec) on the logarithmic scale for the Problem 5.6.

Problem 5.7. Consider the following nonlinear two-body system taken from [16]:

$$v_1''(x) = \frac{-v_1(x)}{r^3}, \qquad v_1(0) = 1, \qquad v_1'(0) = 0,$$
$$v_2''(x) = \frac{-v_2(x)}{r^3}, \qquad v_2(0) = 0, \qquad v_2'(0) = 1,$$
$$r = \sqrt{v_1(x)^2 + v_2(x)^2}, \qquad 0 \leqslant x \leqslant 200, \qquad \omega = 2\pi.$$

The exact solution is $v_1(x) = \cos(x)$, $v_2(x) = \sin(x)$. The above two-body nonlinear system is simulated with the optimized $\mathcal{A}$-stable hyperbolically fitted method given in (2.10) and other existing methods while taking different values for the number of steps N using constant strategies. As observed in Tables 21-23, the proposed approach (OAHFM) returned the smallest values of the absolute errors and highest values for the precision factors, leading to prove its better performance in comparison to other methods. It has

further been noted in Tables 21-23 that the methods (FESDIRK, Rad-II,) did not return the acceptable value of the precision factor owing to having comparatively largest errors.

Table 21: The error distributions and the precision factor (scd) for the Problem 5.7 with number of steps $N = 1000$ using constant stepsize h.

Method	$\|NE\|_\infty$	RMSE	Mean	scd
OAHFM	3.0637×10^{-3}	3.0428×10^{-3}	3.0427×10^{-3}	2.5138
Jator	1.1497×10^{-1}	1.1417×10^{-1}	1.1417×10^{-1}	0.0939
FESDIRK	1.1122×10^{4}	6.9624×10^{3}	4.9031×10^{3}	-4.046
Rad-II	2.8589×10^{5}	2.0263×10^{5}	1.5292×10^{5}	-5.456

Table 22: The error distributions and the precision factor (scd) for the Problem 5.7 with number of steps $N = 2000$ using constant stepsize h.

Method	$\|NE\|_\infty$	RMSE	Mean	scd
OAHFM	2.2442×10^{-4}	2.227×10^{-4}	2.227×10^{-4}	3.649
Jator	7.0267×10^{-3}	6.9723×10^{-3}	6.9722×10^{-3}	2.153
FESDIRK	3.7431×10^{2}	1.873×10^{2}	9.8387×10^{1}	-2.573
Rad-II	1.5314×10^{5}	1.092×10^{5}	8.6561×10^{4}	-5.185

Table 23: The error distributions and the precision factor (scd) for the Problem 5.7 with number of steps $N = 4000$ using constant stepsize h.

Method	$\|NE\|_\infty$	RMSE	Mean	scd
OAHFM	2.1636×10^{-5}	2.1474×10^{-5}	2.1473×10^{-5}	4.665
Jator	4.365×10^{-4}	4.3321×10^{-4}	4.332×10^{-4}	3.360
FESDIRK	8.8814×10^{2}	4.5275×10^{2}	2.6814×10^{2}	-2.949
Rad-II	8.6622×10^{4}	6.2858×10^{4}	5.3306×10^{4}	-4.938

Problem 5.8. The catenary equation is the mathematical description of the curve formed by a flexible, uniform cable or chain hanging freely between two points under the influence of gravity. The equation is given by:

$$v(x) = a\cosh(x/a),$$

where v is the vertical distance from the lowest point of the cable, x is the horizontal distance from the lowest point of the cable, a is the constant parameter that determines the shape of the curve, and cosh is the hyperbolic cosine function. The associated initial value problem for the catenary equation involves finding the specific solution that satisfies certain conditions at the endpoints of the cable. For example, if the cable is hanging between two points (x_1, v_1) and (x_2, v_2), the initial conditions could be: $v(x_1) = v_1$, $v(x_2) = v_2$. These conditions specify the position of the cable at the endpoints, which in turn determines the value of the constant parameter a. Once the value of a is known, the entire shape of the cable can be determined using the catenary equation. Consider the following well-known second-order IVP that produces catenary curve [30]:

$$v''(x) = \sqrt{1+v'(x)^2}, \quad v(0) = 1, \ v'(0) = 0, \quad x \in [0, 10], \quad \omega = 5\pi. \tag{5.4}$$

The exact solution (catenary curve) is given as $v(x) = \cosh(x)$. The Eq. (5.4) is simulated with the optimized $\mathcal{A}$-stable hyperbolically fitted method given in (2.10) and other existing methods while taking different values for the number of steps N using both constant and adaptive stepsize strategies. As observed in Tables 24-26, the proposed approach (OAHFM) returned the smallest values of the absolute

errors and highest values for the precision factors, leading to prove its better performance in comparison to other methods.

Table 24: The error distributions and the precision factor (scd) for the Problem 5.8 with number of steps N = 500 using constant stepsize h.

Method	$\|\|NE\|\|_\infty$	RMSE	Mean	scd
OAHFM	1.1211×10^{-4}	1.1211×10^{-4}	1.1211×10^{-4}	3.950
Jator	5.3182×10^{-3}	5.3181×10^{-3}	5.3181×10^{-3}	2.274
FESDIRK	1.4363×10^{-3}	1.4363×10^{-3}	1.4363×10^{-3}	2.843
Rad-II	8.8996×10^{-3}	8.8995×10^{-3}	8.8995×10^{-3}	2.051

Table 25: The error distributions and the precision factor (scd) for the Problem 5.8 with number of steps N = 1000 using constant stepsize h.

Method	$\|\|NE\|\|_\infty$	RMSE	Mean	scd
OAHFM	3.1974×10^{-5}	3.1974×10^{-5}	3.1974×10^{-5}	4.495
Jator	3.3154×10^{-4}	3.3154×10^{-4}	3.3154×10^{-4}	3.480
FESDIRK	1.795×10^{-4}	1.795×10^{-4}	1.795×10^{-4}	3.746
Rad-II	1.1151×10^{-3}	1.1151×10^{-3}	1.1151×10^{-3}	2.953

Table 26: The error distributions and the precision factor (scd) for the Problem 5.8 with number of steps N = 2000 using constant stepsize h.

Method	$\|\|NE\|\|_\infty$	RMSE	Mean	scd
OAHFM	8.2185×10^{-6}	8.2185×10^{-6}	8.2185×10^{-6}	5.085
Jator	2.0991×10^{-5}	2.0991×10^{-5}	2.0991×10^{-5}	4.678
FESDIRK	2.2435×10^{-5}	2.2435×10^{-5}	2.2435×10^{-5}	4.649
Rad-II	1.3955×10^{-4}	1.3955×10^{-4}	1.3955×10^{-4}	3.855

6. Conclusion with future directions

In this paper, we propose an optimized $\mathcal{A}$-stable hyperbolically fitted method (OAHFM), which can be used to get reliable approximate solutions to IVPs that arise in a variety of scientific and engineering fields as mathematical models. This method can be used efficiently to get these approximate solutions. The OAHFM method evaluates the solution at both the endpoint and the intermediate point by taking into account one intermediate (off-grid) location that has been chosen appropriately by optimizing the amount of local truncation error. According to the results of the numerical simulations that were discussed in the previous part, the OAHFM is more effective than the other available numerical methods that were used for comparison. An intriguing question that will be investigated in subsequent work is how to use the suggested method to solve integrodifferential and partial differential equations. This is a topic that has a lot of potential.

Acknowledgment

We extend our sincerest gratitude to the peers and the reviewers for their critical analysis and constructive feedback which greatly contributed to the success of this work.

References

[1] R. I. Abdulganiy, O. A. Akinfenwa, H. Ramos, S. A. Okunuga, *A second-derivative functionally fitted method of maximal order for oscillatory initial value problems*, Comput. Appl. Math., **40** (2021), 18 pages. 2, 3.2, 3.3, 5.4

[2] M. Adel, M. M. Khader, H. Ahmad, T. A. Assiri, *Approximate analytical solutions for the blood ethanol concentration system and predator-prey equations by using variational iteration method*, AIMS Math., **8** (2023), 19083–19096. 1

[3] M. Adel, K. U. Tariq, H. Ahmad, S. M. R. Kazmi, *Soliton solutions, stability, and modulation instability of the (2+ 1)-dimensional nonlinear hyperbolic Schrödinger model*, Opt. Quantum Electron., **56** (2024). 1

[4] S. Afzal, M. Qayyum, A. Akgül, A. M. Hassan, *Heat transfer enhancement in engine oil based hybrid nanofluid through combustive engines: An entropy optimization approach*, Case Stud. Therm. Eng., **52** (2023), 16 pages. 1

[5] H. Ahmad, M. N. Khan, I. Ahmad, M. Omri, M. F. Alotaibi, *A meshless method for numerical solutions of linear and nonlinear time-fractional Black-Scholes models*, AIMS Math., **8** (2023), 19677–19698. 1

[6] H. Ahmad, D. U. Ozsahin, U. Farooq, M. A. Fahmy, M. D. Albalwi, H. Abu-Zinadah, *Comparative analysis of new approximate analytical method and Mohand variational transform method for the solution of wave-like equations with variable coefficients*, Results Phys., **51** (2023), 10 pages. 1

[7] O. A. Akinfenwa, R. I. Abdulganiy, B. I. Akinnukawe, S. A. Okunuga, *Seventh order hybrid block method for solution of first order stiff systems of initial value problems*, J. Egyptian Math. Soc., **28** (2020), 11 pages. 3.3

[8] K. K. Ali, S. Tarla, M. R. Ali, A. Yusuf, R. Yilmazer, *Physical wave propagation and dynamics of the Ivancevic option pricing model*, Results Phys., **52** (2023), 10 pages. 1

[9] K. K. Ali, S. Tarla, A. Yusuf, *Quantum-mechanical properties of long-lived optical pulses in the fourth-order KdV-type hierarchy nonlinear model*, Opt. Quantum Electron., **55** (2023).

[10] K. K. Ali, A. Yusuf, M. Alquran, S. Tarla, *New physical structures and patterns to the optical solutions of the nonlinear Schrödinger equation with a higher dimension*, Commun. Theor. Phys. (Beijing), **75** (2023).

[11] M. Alquran, T. A. Sulaiman, A. Yusuf, A. S. Alshomrani, D. Baleanu, *Nonautonomous lump-periodic and analytical solutions to the (3+ 1)-dimensional generalized Kadomtsev–Petviashvili equation*, Nonlinear Dyn., **111** (2023), 11429–11436. 1

[12] J. C. Butcher, *Numerical methods for ordinary differential equations*, John Wiley & Sons, Ltd., Chichester, (2016). 5, 5.2

[13] M. S. H. Chowdhury, I. Hashim, S. Momani, *The multistage homotopy-perturbation method: A powerful scheme for handling the Lorenz system*, Chaos Solitons Fractals, **40** (2009), 1929–1937. 5.5

[14] Z. Eskandari, P. A. Naik, M. Yavuz, *Dynamical behaviors of a discrete-time preypredator model with harvesting effect on the predator*, J. Appl. Anal. Comput., **14** (2024), 283–297. 1

[15] W. A. Faridi, Z. Myrzakulova, R. Myrzakulov, A. Akgül, M. S. Osman, *The construction of exact solution and explicit propagating optical soliton waves of Kuralay equation by the new extended direct algebraic and Nucci's reduction techniques*, Int. J. Model. Simul., (2024), 1–20. 1

[16] F. A. Fawzi, N. Senu, F. Ismail, Z. A. Majid, *New phase-fitted and amplification-fitted modified Runge-Kutta method for solving oscillatory problems*, Glob. J. Pure Appl. Math., **12** (2016), 1229–1242. 5.7

[17] E. Hairer, S. P. Nørsett, G. Wanner, *Solving ordinary differential equations. I*, Springer-Verlag, Berlin, (1993). 1

[18] E. Harier, G. Wanner, *Solving ordinary differential equations. II*, Springer-Verlag, Berlin, (2010). 1, 5.1

[19] M. S. Hashemi, M. Mirzazadeh, H. Ahmad, *A reduction technique to solve the (2+ 1)-dimensional KdV equations with time local fractional derivatives*, Opt. Quantum Electron., **55** (2023). 1

[20] P. Henrici, *Discrete variable methods in ordinary differential equations*, John Wiley & Sons, New York-London, (1962). 1

[21] N. Kaid, A. Akgul, M. A. Alkhafaji, K. S. Mohsen, J. Asad, R. Jarrar, H. Shanak, Y. Menni, S. Abdullaev, *CFD simulation and optimization of heat transfer enhancement in HEV static mixers with rotated angles for turbulent flows*, Therm. Sci., **27** (2023), 3123–3131. 1

[22] Z. Kalogiratou, Th. Monovasilis, H. Ramos, T. E. Simos, *A new approach on the construction of trigonometrically fitted two step hybrid methods*, J. Comput. Appl. Math., **303** (2016), 146–155. 1

[23] S. Khaliq, S. Ahmad, A. Ullah, H. Ahmad, S. Saifullah, T. A. Nofal *New waves solutions of the (2+ 1)-dimensional generalized Hirota–Satsuma–Ito equation using a novel expansion method*, Results Phys., **50** (2023), 5 pages. 1

[24] S. A. Khan, S. Yasmin, H. Waqas, E. A. Az-Zo'bi, A. Alhushaybari, A. Akgül, A. M. Hassan, M. Imran, *Entropy optimized ferro-copper/blood based nanofluid flow between double stretchable disks: Application to brain dynamic*, Alexandria Eng. J., **79** (2023), 296–307. 1

[25] M. C. Korti, A. Youcef, A. Akgul, A. A. Alwan, K. S. Mohsen, J. Asad, R. Jarrar, H. Shanak, Y. Menni, S. H. Abdullaev, *Optimizing solar water heater performance through a numerical study of zig-zag shaped tubes*, Therm. Sci., **27** (2023), 3143–3153. 1

[26] A. A. Kosti, Z. A. Anastassi, T. E. Simos, *Construction of an optimized explicit Runge-Kutta-Nyström method for the numerical solution of oscillatory initial value problems*, Comput. Math. Appl., **61** (2011), 3381–3390. 5.3

[27] J. D. Lambert, *Computational methods in ordinary differential system*, John Wiley & Sons, London, New York, (1973). 3.1

[28] J. D. Lambert, *Numerical methods for ordinary differential systems*, John Wiley & Sons, Ltd., Chichester, (1991). 3.1

[29] S. Li, S. Ullah, S. A. AlQahtani, S. M. Tag, A. Akgül, *Mathematical assessment of Monkeypox with asymptomatic infection: Prediction and optimal control analysis with real data application*, Results Phys., **51** (2023), 14 pages. 1

[30] L. Martínez-Jiménez, J. M. Cruz-Duarte, J. J. Rosales-García, *Fractional solution of the catenary curve*, Math. Methods Appl. Sci., **44** (2021), 7969–7978. 5.8
[31] S. F. Megahid, A. E. Abouelregal, H. Ahmad, M. A. Fahmy, H. Abu-Zinadah, *A generalized More-Gibson-Thomson heat transfer model for the study of thermomagnetic responses in a solid half-space*, Results Phys., **51** (2023), 11 pages. 1
[32] P. A. Naik, M. Amer, R. Ahmed, S. Qureshi, Z. Huang, *Stability and bifurcation analysis of a discrete predator-prey system of Ricker type with refuge effect*, Math. Biosci. Eng., **21** (2024), 4554–4586. 1
[33] F. F. Ngwane, S. N. Jator, *Block hybrid method using trigonometric basis for initial value problems with oscillating solutions*, Numer. Algorithms, **63** (2013), 713–725. 5
[34] S. Ola Fatunla, *Block methods for second order ODEs*, Int. J. Comput. Math., **41** (1991), 55–63. 3.2
[35] K. Ozawa, *A functionally fitted three-stage explicit singly diagonally implicit Runge-Kutta method*, Japan J. Indust. Appl. Math., **22** (2005), 403–427. 5
[36] M. Qayyum, E. Ahmad, S. T. Saeed, H. Ahmad, S. Askar, *Homotopy perturbation method-based soliton solutions of the time-fractional (2+ 1)-dimensional Wu–Zhang system describing long dispersive gravity water waves in the ocean*, Front. Phys., **11** (2023), 12 pages. 1
[37] M. Qayyum, E. Ahmad, S. T. Saeed, A. Akgül, S. M. El Din, *New solutions of fractional 4d chaotic financial model with optimal control via he-laplace algorithm*, Ain Shams Eng. J., **15** (2024), 10 pages. 1
[38] S. Qureshi, H. Ramos, A. Soomro, E. Hincal, *Time-efficient reformulation of the Lobatto III family of order eight*, J. Comput. Sci., **63** (2022). 1
[39] H. Ramos, M. A. Rufai, *An adaptive one-point second-derivative Lobatto-type hybrid method for solving efficiently differential systems*, Int. J. Comput. Math., **99** (2002), 1687–1705. 1
[40] H. Ramos, S. Qureshi, A Soomro, *Adaptive step-size approach for Simpson's-type block methods with time efficiency and order stars*, Comput. Appl. Math., **40** (2021), 20 pages. 4
[41] H. Ramos, M. A. Rufai, *A two-step hybrid block method with fourth derivatives for solving third-order boundary value problems*, J. Comput. Appl. Math., **404** (2022), 21 pages. 1
[42] H. Ramos, G. Singh, *A note on variable step-size formulation of a Simpson's-type second derivative block method for solving stiff systems*, Appl. Math. Lett., **64** (2017), 101–107. 4
[43] H. Ramos, G. Singh, *Solving second order two-point boundary value problems accurately by a third derivative hybrid block integrator*, Appl. Math. Comput., **421** (2022), 19 pages. 1
[44] Q. Raza, X. Wang, M. Z. Akbar Qureshi, I. Siddique, M. Ahmad, B. Ali, H. Ahmad, F. Tchier, *Significance role of dual porosity and interfacial nanolayer mechanisms on hybrid nanofluids flow: a symmetry flow model*, Mod. Phys. Lett. B, **38** (2024). 1
[45] A. E. Sedgwick, *AN EFFECTIVE VARIABLE-ORDER VARIABLE-STEP ADAMS METHOD*, ProQuest LLC, Ann Arbor, MI, (1973). 4
[46] G. Singh, A. Garg, V. Kanwar, H. Ramos, *An efficient optimized adaptive step-size hybrid block method for integrating differential systems*, Appl. Math. Comput., **362** (2019), 10 pages. 4
[47] E. Stiefel, D. G. Bettis, *Stabilization of Cowell's method*, Numer. Math., **13** (1969), 154–175. 5.6
[48] T. A. Tarray, P. A. Naik, R. A. Najar, *Matrix representation of an all-inclusive Fibonacci sequence*, Asian J. Math. Stat., **11** (2018), 18–26. 1
[49] A. Tassaddiq, S. Qureshi, A. Soomro, E. Hincal, A. A. Shaikh, *A new continuous hybrid block method with one optimal intrastep point through interpolation and collocation*, Fixed Point Theory Algorithms Sci. Eng., **2022** (2022), 17 pages. 3.3
[50] I. Ullah, A. Ullah, S. Ahmad, H. Ahmad, T. A. Nofal, *A survey of KdV-CDG equations via nonsingular fractional operators*, AIMS Math., **8** (2023), 18964–18981. 1
[51] J. Vigo-Aguiar, H. Ramos, *A strategy for selecting the frequency in trigonometrically-fitted methods based on the minimization of the local truncation errors and the total energy error*, J. Math. Chem., **52** (2014), 1050–1058. 5
[52] G. M. Vijayalakshmi, P. Roselyn Besi, A. Akgül, *Fractional commensurate model on COVID-19 with microbial co-infection: An optimal control analysis*, Optim. Control Appl. Methods, **45** (2024), 1108–1121. 1
[53] H. A. Watts, *Starting step size for an ODE solver*, J. Comput. Appl. Math., **9** (1983), 177–191. 4
[54] L. Zada, I. Ullah, R. Nawaz, W. Jamshed, E. N. Saddam, S. A. Idris, H. Ahmad, A. Amjad, *Computational treatment and thermic case study of entropy resulting from nanofluid flow of convergent/divergent channel by applying the lorentz force*, Case Stud. Therm. Eng., **54** (2024), 12 pages. 1
[55] Zil-E-Huma, A. R. Butt, N. Raza, H. Ahmad, D. U. Ozsahin, F. Tchier, *Different solitary wave solutions and bilinear form for modified mixed-KDV equation*, Optik, **287** (2023). 1